Supplemental Text (p-values)

Figure	Group 1	Group 2	p-Value, Student 2-tailed
1B	2E4 non-irradiated MAC1+	2.5E5 irradiated MAC1+	0.0076
1B	2E4 non-irradiated B220+	2.5E5 irradiated B220+	0.0063
2A	no IR control	3d post IR	0.0036
2A	no IR control	1w post IR	0.0061
2A	no IR control	3w post IR	<0.0001
2A	no IR control	3d post IR + NAC	0.95
2A	no IR control	1w post IR + NAC	0.9
2A	no IR control	3w post IR + NAC	0.38
2A	3d post IR	3d post IR + NAC	0.0071
2A	1w post IR	1w post IR + NAC	0.0238
2A	3w post IR	3w post IR + NAC	0.007
3B	no IR control	2 hrs post IR	<0.0001
3B	7d post IR	7d post IR + NAC	0.0136
4	BCR-ABL non IR total	BCR-ABL IR total	0.0099
4	BCR-ABL non IR B220+	BCR-ABL IR B220+	0.0004
4	RAS non IR total	RAS IR total	0.0027
4	RAS non IR MAC1+	RAS IR MAC1+	0.0029
4	RAS non IR B220+	RAS IR B220+	0.0011
4	ICN non IR B220+	ICN IR B220+	0.0336
5	Bcr-Abl IR	Bcr-Abl non IR	0.0042
5	RAS non IR	RAS IR	0.0015
5	ICN non IR	ICN IR	0.0035
6A	control ICN + control comp	IR ICN + IR comp	0.0013
6A	IR ICN + IR comp	IR ICN + control comp	0.0014
6B	control ICN + control comp	IR ICN + IR comp	0.035
6B	IR ICN + IR comp	IR ICN + control comp	0.0034
6D	control ICN + control comp	control ICN + IR comp	0.043
6D	control ICN + control comp	IR ICN + IR comp	<0.0001
6D	IR ICN + IR comp	IR ICN + control comp	<0.0001

Supplementary Figure Legends:

Supplementary Figure S1. Hematopoiesis has returned to steady state by 6 weeks after sublethal irradiation. Mice were irradiated with 5 Gy or mock-irradiated. Six weeks later the animals were sacrificed. Concentrations of red blood cells (RBC) and white blood cells (WBC) in the peripheral blood were determined by automated complete blood counts (CBC) using a Cell Dyn 1700 automated cell counter. Tibia cellularity was determined by cell counting using a Quanta cytometer. Spleens were weighed. Each dot represents an individual mouse.

Supplementary Figure S2. Reductions in BM progenitor cell fitness by X-irradiation are evident within one week of irradiation.

BM was isolated from Balb/c mice that have been irradiated 1 week before with 5 Gy (or not as the control), and then mixed with BM from non-irradiated GFP-Tg animals at 9:1 ratios. The mixes were then transplanted into lethally irradiated mice at 10^7 cells/recipient. At 2 month post-irradiation, peripheral blood was collected, stained with PE-Cy7-anti-GR1 plus PE-anti-B220 antibodies, and analyzed for the percentages of GFP^+ cells in the indicated blood lineages by flow cytometry.

Supplementary Figure S3. Effects of NAC treatment of hematopoietic fitness as assessed by competition with unirradiated BM. Mice maintained on a water supply with or without 40μM NAC for 3 days (*NAC before IR*) were irradiated at 5 Gy, and transferred to cages with regular water or with water supplemented with 40μM NAC

(*NAC after IR*), as indicated. At 6 weeks post irradiation, BM was harvested (Test BM) and mixed with BM from unirradiated GFP-Tg animal, at 19:1 proportion of Test/GFP-Tg viable cells. The mixes were transplanted into lethally irradiated animals at $3x10^6$ cells per recipient. Peripheral blood was analyzed at 3 weeks **(A)** and 10 weeks **(B)** post transplantation for GFP expression in the indicated lineages as in Figure 1B. Three weeks after transplantation, when contributions to peripheral blood largely reflects short-term hematopoietic progenitor activity, we observed a greater ability of irradiated BM to compete with unirradiated GFP-Tg BM for reconstitution of both myeloid and B cell lineages when the irradiated BM came from mice treated with NAC either after or before irradiation **(B)**. However, by 10 weeks post-transplant, significant effects of NAC treatment post-irradiation were only observed in the B cell lineage but not the myeloid lineage **(C)**, the latter of which provides a better readout of HSC activity (1). As expected, when NAC treatment was started before irradiation, a substantial fraction of GFP negative cells in both lineages were present even at 10 weeks post irradiation, indicating a significant maintenance of fitness.

Supplementary Figure S4. The numbers of phenotypic HSC are not significantly affected by previous irradiation. BM from Balb/c mice irradiated 6 weeks prior was harvested and stained with APC-anti-Ter119, APC-anti-GR-1, APC-anti-CD3, APC-anti-B220 (together representing the APC-Lin stain), PE-Cy7-anti-Sca1, PE-anti-CD34, PE-anti-Flk2 and FITC-anti-cKit. The cells were analyzed for the percentages of KSL and KSL $CD34^{neg}FLK2^{neg}$ populations. **A)** Gating schemata for KSL $CD34^{neg}FLK2^{neg}$ cells, represented in the R6 gate. KSL cells are represented in the combined R4 and R6 gates.

B) Percentages of KSL and KSL $CD34^{neg}FLK2^{neg}$ cells. Each dot represents an individual mouse.

Supplementary Figure S5. Irradiation reduces the numbers of functional HSC, but does not affect homing to the BM. A) For the limiting dilution assays shown in Figure 1B, concentrations of functional HSC were determined with the L-Calc^{TM} program from Stem Cell Technologies. The numbers of functional HSC were determined based on the ability of different doses of BM to contribute to hematopoiesis in both the myeloid ($Mac1^{+}$) and B-cell ($B220^{+}$) lineages (with ≥1% contribution required to be scored as positive). The P value for statistical difference between irradiated and non-irradiated groups is less than 0.0001. **B)** The numbers of phenotypic HSCs ($CD150^{+}Lineage^{neg}CD48^{neg}$ cells) per tibia were determined in the BM of mice irradiated 6 weeks prior at 5 Gy (or not irradiated as the control) by flow cytometry. $CD150^{+}CD48^{neg}Lineage^{neg}$ cells in the BM have been shown to be highly enriched for HSC (2). 10^{7} cells from each of the 4 donors (2 previously irradiated and 2 control) were then transplanted into each recipient mouse, with 2 mice per donor. Numbers of phenotypic HSC per tibia (shown per tibia) were then determined at 2 days post-transplantation as above. **C)** The percentages of phenotypic HSC in the same mice are shown.

Supplementary Figure S6. Mice were left untreated (-) or irradiated with 5 Gy (+), and then maintained on water with or without 40 μM NAC (starting after irradiation). At 48 hours, 1 week or 6 weeks after irradiation, mice were sacrificed, and BM and peripheral

blood were isolated and counted. **A)** Micronuclei in reticulocytes (MN-RET) were determined by staining whole heparinized blood with anti-CD71-Fitc and propidium iodide (PI) as previously described (3-5). The MN-RET is an established assay for the detection of irradiation induced strand breaks in hematopoietic progenitors (5). **B)** BM cellularity using the Quanta flow cytometer (see Supplementary Figure 1 for the 6 week time point). **C)** Harvested BM was stained with Krishan's buffer (0.1% sodium citrate, 50 μg/mL propidium iodide, 20 μg/mL RNase A, 0.5% NP40), and cell cycle phasing determined by flow cytometric analysis of PI staining intensity. The fraction of cells in the sub-G1, G1, S and G2 phases are plotted. Irradiation led to decreased fractions of cells in S phase at 48 hours, as well as an increased fraction of cells with sub-G1 DNA content (indicative of apoptosis) which persisted for at least 6 weeks. **D)** BM cells were resuspended in RIPA buffer, and equal cell numbers ($2x10^6$) were electrophoresed on a 4-20% gradient polyacrylamide gel, and then western blotted using antibodies against p53 (Oncogene Ab-3, OP29-100UG) and Actin (Santa Cruz I-19, sc-1616). Note that modest and persistent increases in p53 protein levels are observed after irradiation. Note also that two samples are underloaded. Each lane is derived from a separate mouse.

Supplementary Figure S7. Prior irradiation does not affect the activities of ectopically expressed Bcr-Abl, Ras and Akt. Mice were left untreated (-) or irradiated with 5 Gy (+). Six weeks later, mice were sacrificed, and BM was isolated. The c-Kit^+ BM fraction (early progenitor enriched) was isolated and transduced with MiG vector or MiG expressing activated Akt, p185 Bcr-Abl or N-Ras12D. Cells were then cultured under stem cell conditions (most cells will be KSL within 4 days; not shown), as

previously described (6). After 4 days of culture, the cells were harvested, permeabilized using the Fix and Perm kit following the provided directions (Invitrogen), and analyzed by flow cytometry using phospho-specific antibodies recognizing activating phosphorylation states for Stat5 (catalog #612567), Erk (#612566) and Akt (#558275; all from BD Pharmingen). Flow profiles were gated on the GFP^{+} (green) or GFP^{neg} (red) fractions, and the isotype antibody control is shown in gray.

Supplementary Figure S8. Prior irradiation does not impact upon the expansion of BM progenitors expressing Bcl2.

Mice were left untreated (-) or irradiated with 5 Gy (+). Six weeks later, mice were sacrificed, and BM was isolated and transduced with MiG vector or MiG expressing activated Bcl2, and immediately transplanted into lethally irradiated recipient mice. MiG-Bcl2 was the generous gift of Dr. Scott Lowe (7). Initial transduction efficiencies were determined after 3 days of culture under HSC conditions: 2.33% for unirradiated and 3.86% for irradiated BM cells. At 1 month post-transplantation, peripheral blood was analyzed, and GFP expression was determined within the $MAC1^{+}$ and $B220^{+}$ lineages as in Figure 1B, as well as within total nucleated blood cells. As expected (8), recipients of Bcl2 transduced cells did not develop malignancies within several months.

Supplementary Figure S9. Polyclonal Vβ expression in expanding ICN-expressing T cells. To further distinguish potential contributions of cooperating oncogenic mutations caused by irradiation from changes in the adaptive landscape, we determined the clonality of the expanding ICN^{+} cell population in recipients of previously irradiated BM.

If the observed expansion of ICN-expressing cells were due to random cooperating mutations, the expanding cells would be expected to be a monoclonal population. Spleen cells from mice described in Figure 6C and 6D were stained with antibodies against the indicated Vβ T-cell receptor chain (linked to PE; generous gifts of Dr. Philippa Marrack) and PE-Cy7 linked anti-Mac1 plus PE-Cy7 linked anti-B220. Cells were first gated as $Mac1^{neg}B220^{neg}$, and then analyzed for Vβ and GFP expression. Flow profiles from a single recipient mouse from the IR/ICN+IR-comp group is shown, but similar representation of all tested Vβ chains was observed in the other 4 mice from this group. This method has been previously employed to demonstrate that transplantation of ICN-transduced BM leads to polyclonal extrathymic ICN^+ T-cell expansion, with eventual development of T-ALL with monoclonal Vβ expression (9). The analyses shown here reveal the expression of all of the assayed Vβ chains within the GFP^+ population, indicative of a polyclonal population. In contrast, leukemias that developed at later points were monoclonal (data not shown), indicating that progression from the initial polyclonal expansion to leukemias requires additional events.

Supplementary Figure S10. Examples of flow cytometric gating strategies for the determination of GFP expression within HSC-enriched and $CD4^+CD8^+$ populations in the BM. Gating strategies are shown for the quantitation of GFP^+ cells within the indicated populations used for Figures 6C, 6D and Supplementary Figure S7B. **A, B.** BM was harvested 4 weeks post transplant and stained with PE-anti-Ter119, PE-anti-GR-1, PE-anti-CD3, PE-anti-B220 (together representing the Lin stain), PE-anti-CD48 and APC-CD150. Examples of flow profiles and gating strategies for the

$Lin^{neg}CD48^{neg}CD150^{+}$ HSC-enriched population (elliptical R3 gate) are shown. The percentages of GFP^{+} cells within the HSC-enriched gate are indicated. **C, D.** BM was stained with PacificBlue-linked anti-CD4 and PE-Cy7-anti-CD8. Examples of flow profiles and gating strategies for the $CD4^{+}CD8^{+}$ population are shown. The percentages of $CD4^{+}CD8^{+}$ cells within total BM (circular R28 gate), GFP^{+} cells within the $CD4^{+}CD8^{+}$ population, and GFP^{+} cells within total BM cells (in parentheses) are indicated.

Supplementary Figure S11. The expansion of ICN expressing progenitors in the BM requires a background of irradiated hematopoiesis. Mice were transplanted with MiG-ICN transduced BM as described in Figure 6C and 6D. BM was harvested 4 weeks post transplantation and stained with PE-anti-B220 and PE-Cy7-anti-Mac1, or Pacific Blue linked anti-CD4 and PE-Cy7-anti-CD8. **A.** Selection for ICN expression in the irradiated background results in reduced B-lymphopoiesis. The percentage of $B220^{+}Mac1^{neg}$ cells in the BM for the indicated groups of mice is graphed. **B.** An irradiated background promotes the expansion of ICN-expressing $CD4^{+}CD8^{+}$ (DP) cells in the BM. The percentage of BM cells expressing both GFP and $CD4^{+}CD8^{+}$ is graphed. Similar results were obtained for $CD4^{+}$ and $CD8^{+}$ single positive T-cells in the BM and peripheral blood (data not shown). **C.** Irradiated hematopoiesis selects for ICN expression in the myeloid lineage. The expression of GFP within $Mac1^{+}B220^{neg}$ cells is graphed.

Reference for Supplemental Data:

1. Wright DE, Wagers AJ, Gulati AP, Johnson FL, Weissman IL. Physiological migration of hematopoietic stem and progenitor cells. Science 2001; 294: 1933-6.

2. Yilmaz OH, Kiel MJ, Morrison SJ. SLAM family markers are conserved among hematopoietic stem cells from old and reconstituted mice and markedly increase their purity. Blood 2006; 107: 924-30.
3. Chang PY, Torous D, Lutze-Mann L, Winegar R. Impact of p53 status on heavy-ion radiation-induced micronuclei in circulating erythrocytes. Mutat Res 2000; 466: 87-96.
4. Dertinger SD, Bemis JC, Phonethepswath S, et al. Reticulocyte and micronucleated reticulocyte responses to gamma irradiation: Effect of age. Mutat Res 2009; 675: 77-80.
5. Dertinger SD, Tsai Y, Nowak I, et al. Reticulocyte and micronucleated reticulocyte responses to gamma irradiation: dose-response and time-course profiles measured by flow cytometry. Mutat Res 2007; 634: 119-25.
6. Bilousova G, Marusyk A, Porter CC, Cardiff RD, DeGregori J. Impaired DNA Replication within Progenitor Cell Pools Promotes Leukemogenesis. PLoS Biology 2005; 3: e401.
7. Schmitt CA, Rosenthal CT, Lowe SW. Genetic analysis of chemoresistance in primary murine lymphomas. Nat Med 2000; 6: 1029-35.
8. Harris AW, Strasser A, Bath ML, Elefanty AG, Cory S. Lymphomas and plasmacytomas in transgenic mice involving bcl2, myc and v-abl. Curr Top Microbiol Immunol 1997; 224: 221-30.
9. Li X, Gounari F, Protopopov A, Khazaie K, von Boehmer H. Oncogenesis of T-ALL and nonmalignant consequences of overexpressing intracellular NOTCH1. J Exp Med 2008; 205: 2851-61.

Marusyk_Suppl. Fig. S1

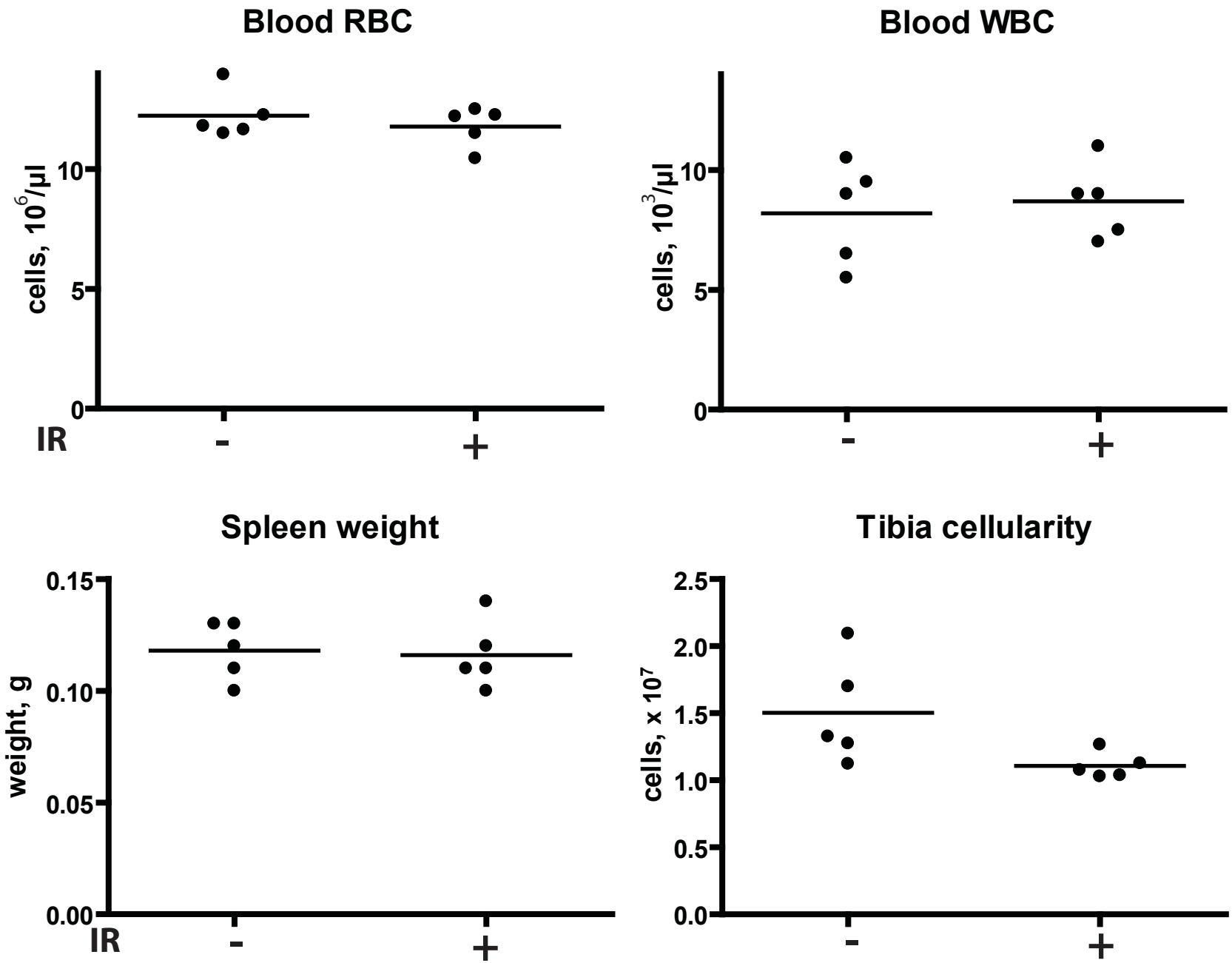

Marusyk_Suppl.Fig.S2

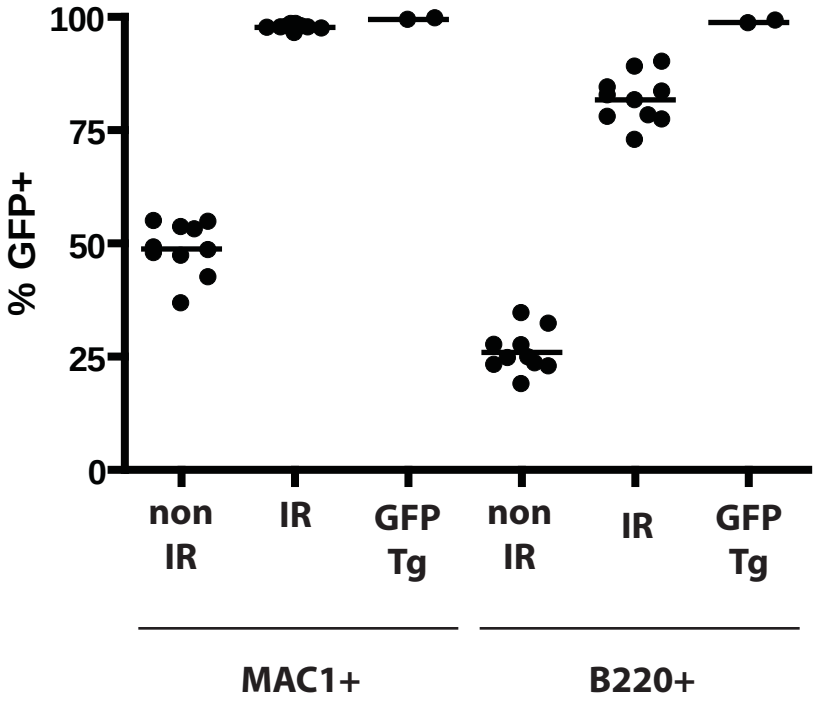

Marusyk_Suppl. Fig. S3

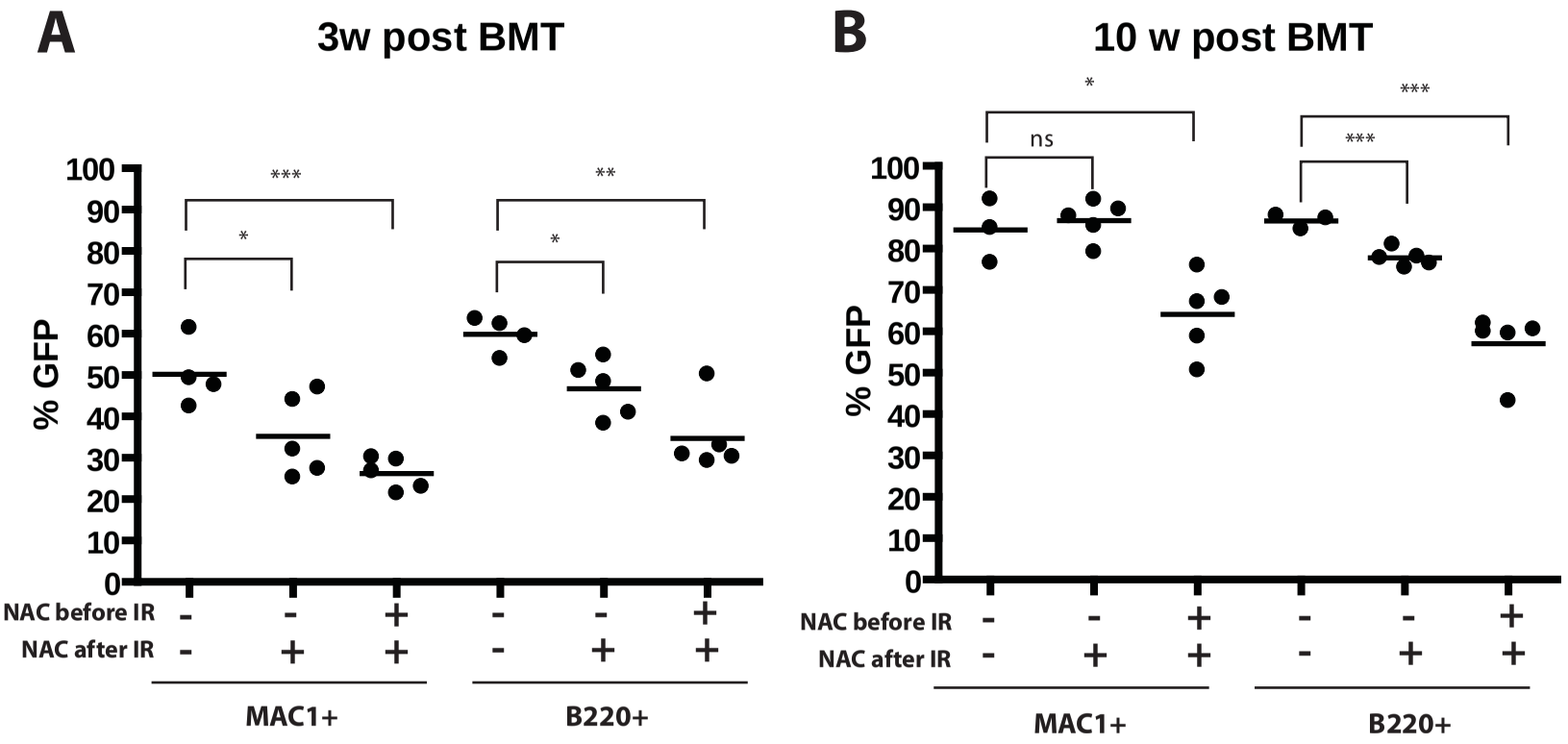

Marusyk_Suppl. Fig. S4

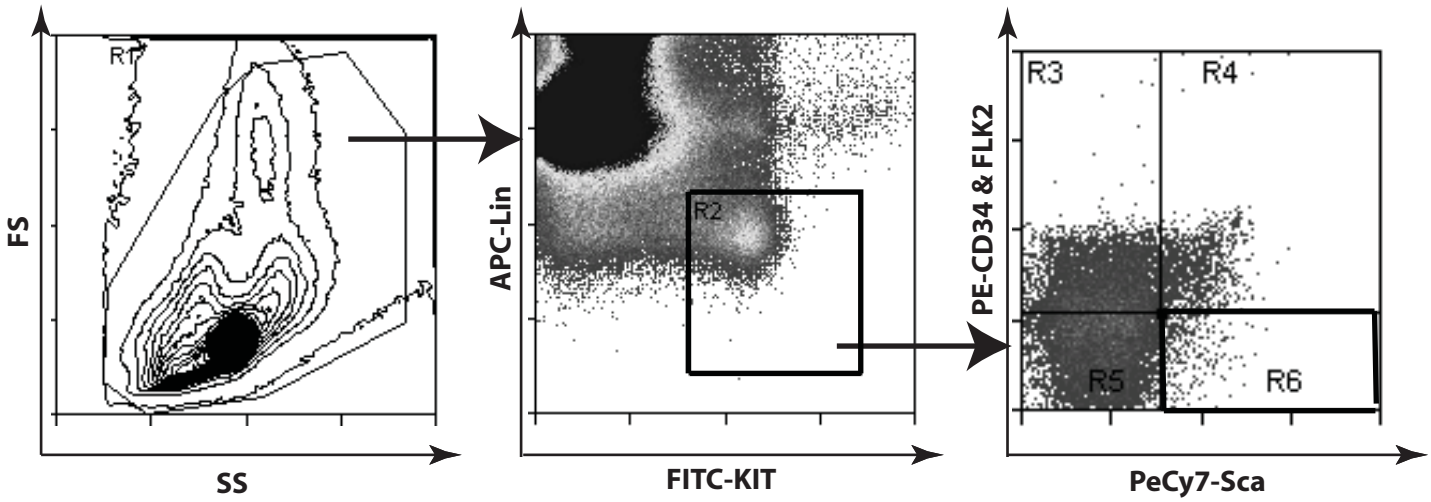

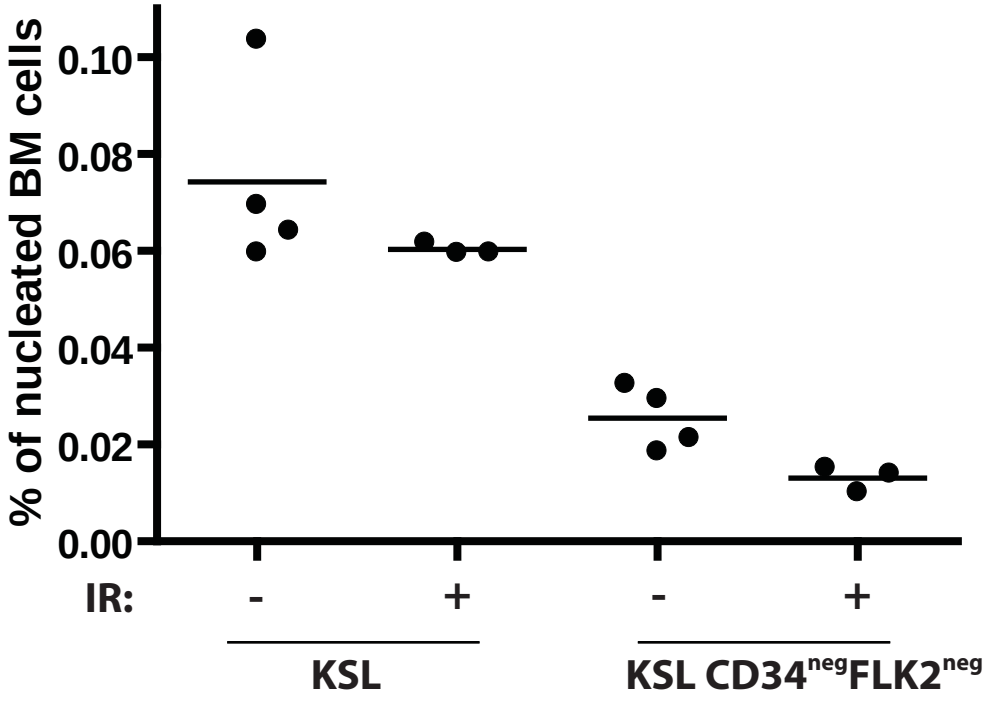

Marusyk_Suppl.Fig.S5

A

	Control			Irradiated		
"test"cells	1E4	2E4	5E4	1E5	2.5E5	5E5
positive/total	3/10	9/10	10/10	7/10	7/10	9/9
HSC frequency 95% confidence interval	1 in 12,702 1 in 7,793 to 1 in 20,704			1 in 133,198 1 in 79,534 to 1 in 223,070		

B

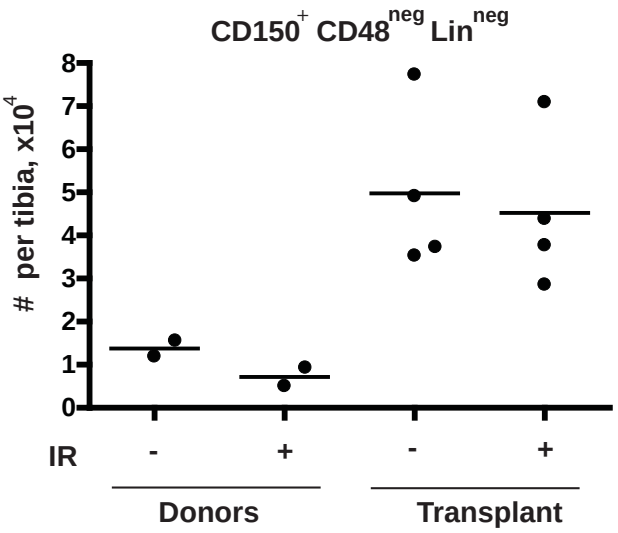

C

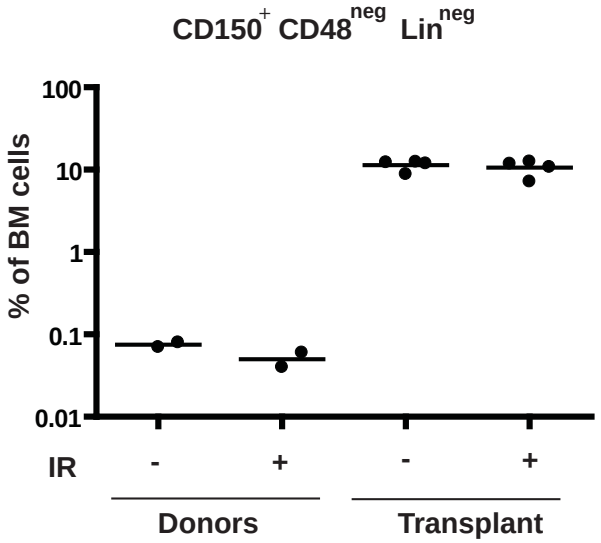

Marusyk_Suppl.Fig.S6

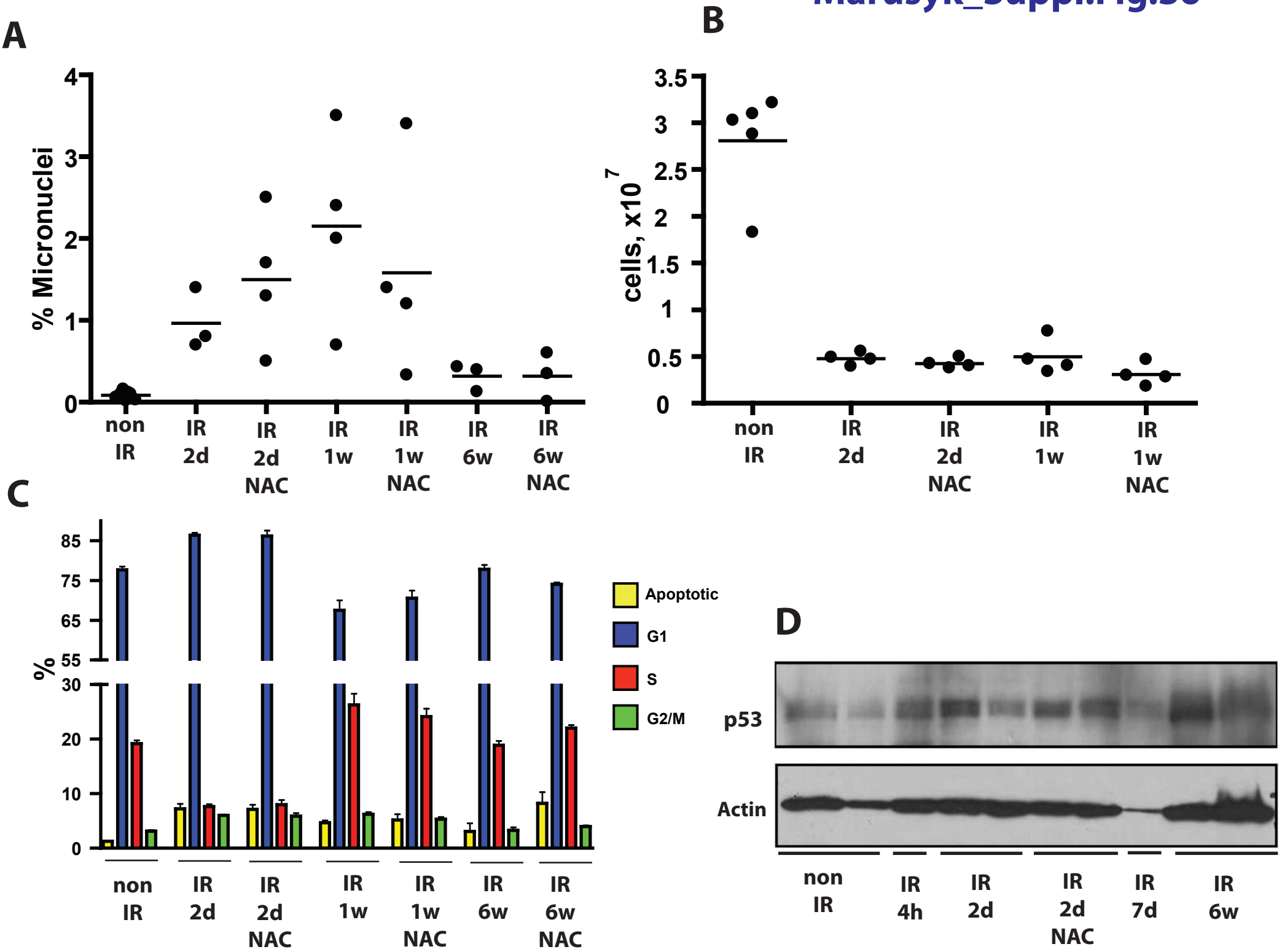

Marusyk_Suppl.Fig.S7

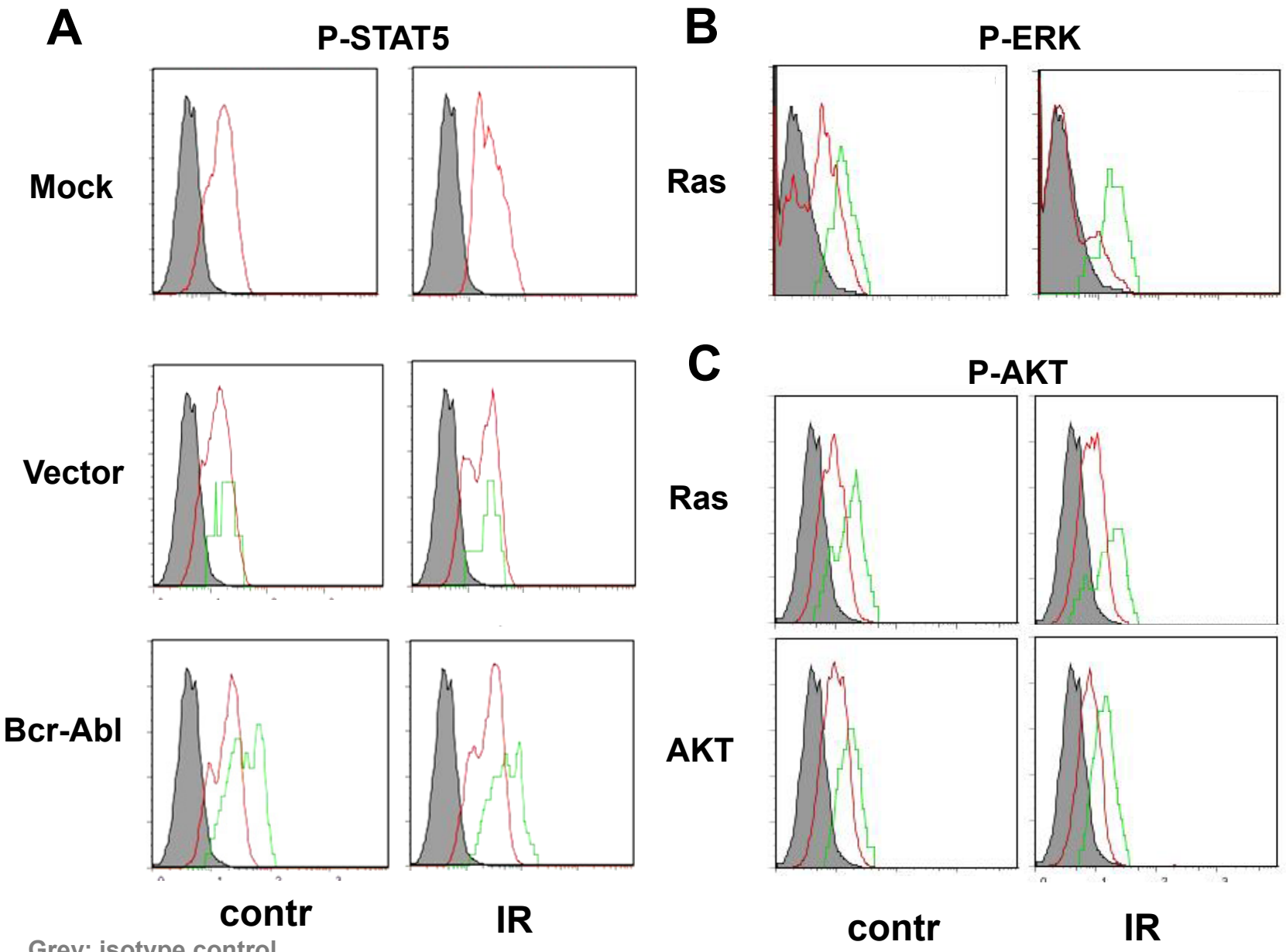

Grey: isotype control
Red: GFP^{neg} cells
Green: GFP^{+} cells

Marusyk_Suppl. Fig. S8

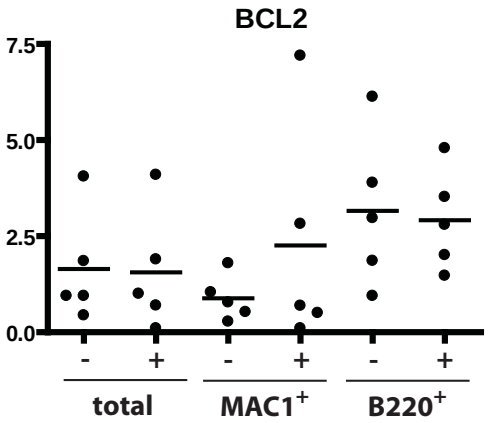

Marusyk_Suppl. Fig. S9

Vβ expression in ICN^{+} splenocytes during short-term expansion

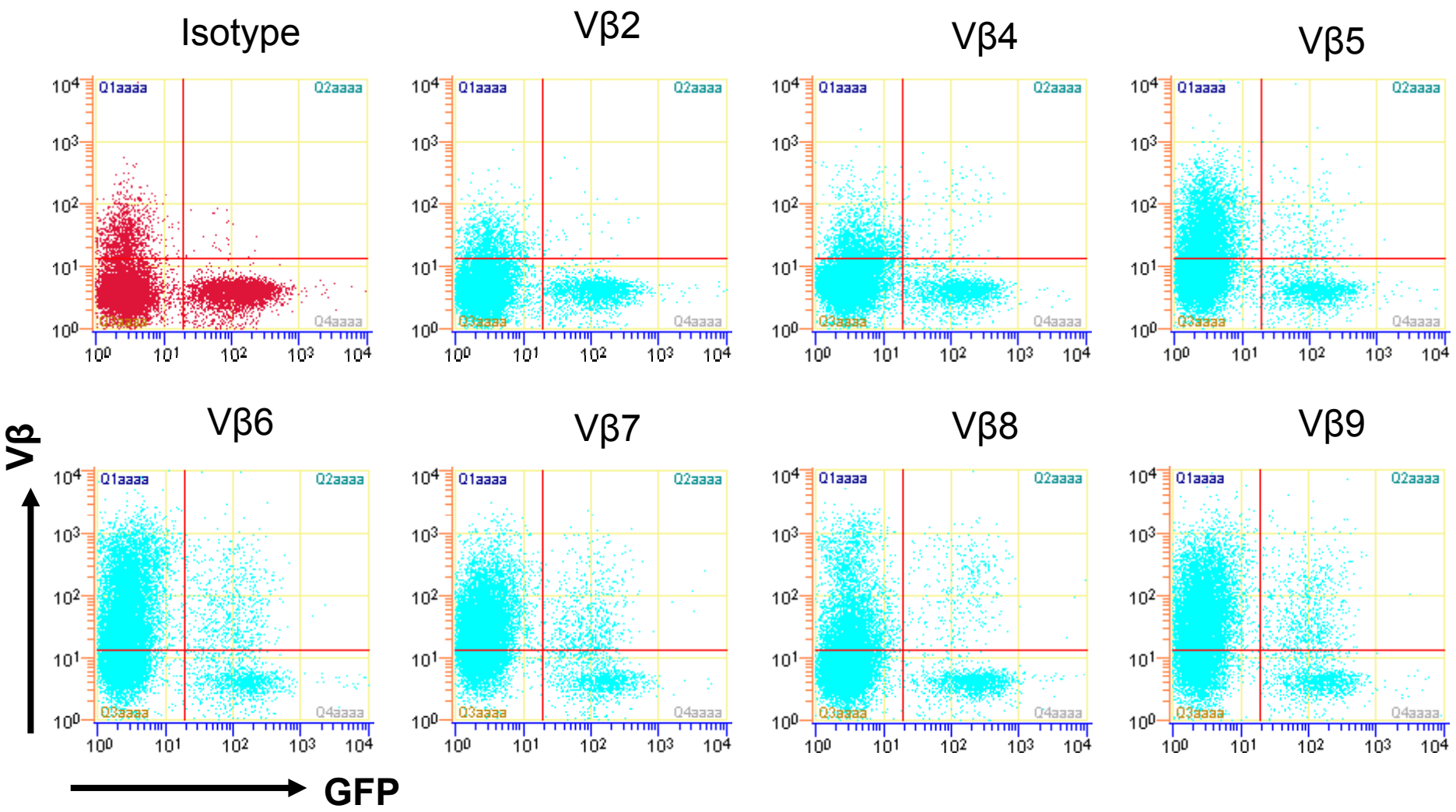

Marusyk_Suppl. Fig. S10A

C/ICN + C-comp

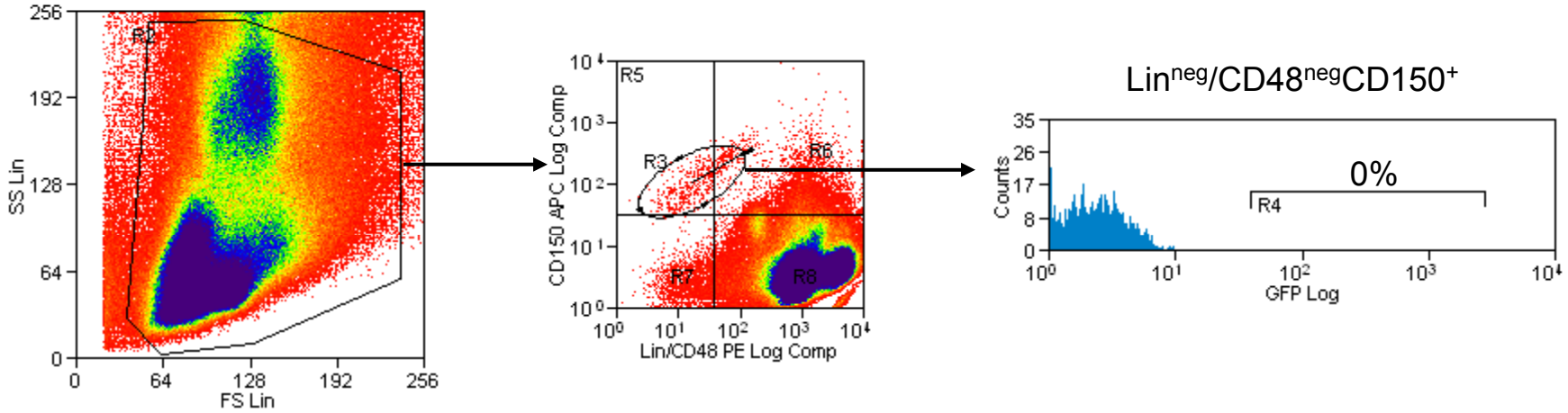

C/ICN + IR-comp

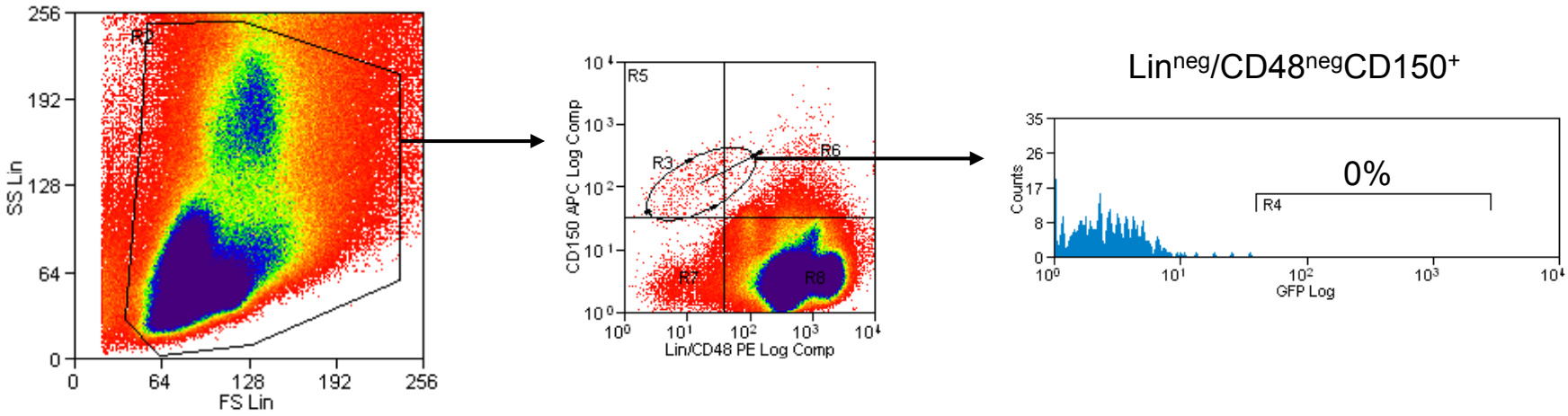

Marusyk_Suppl. Fig. S10B

IR/ICN + C-comp

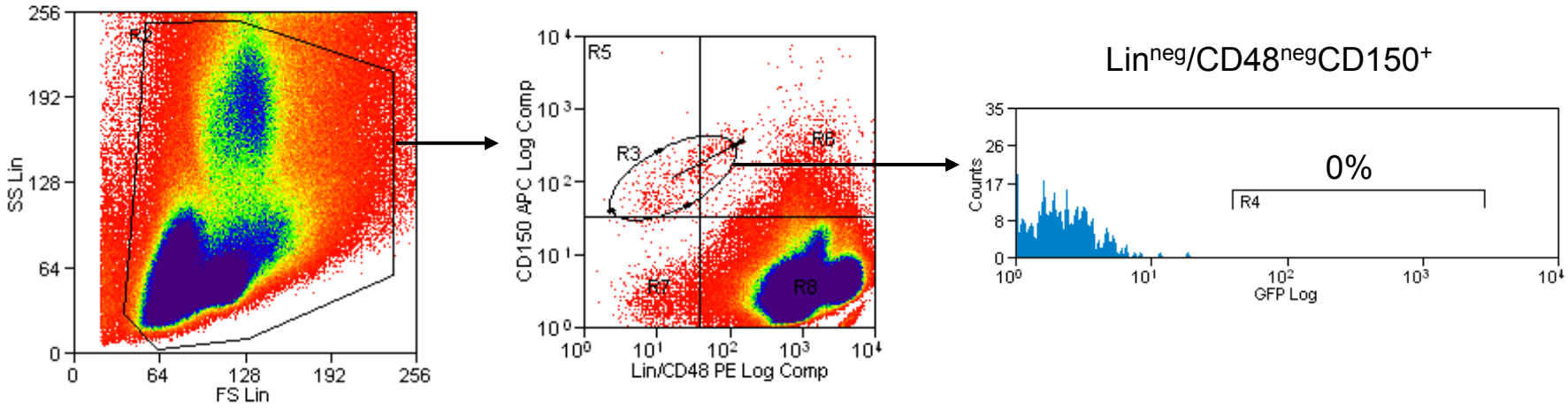

IR/ICN + IR-comp

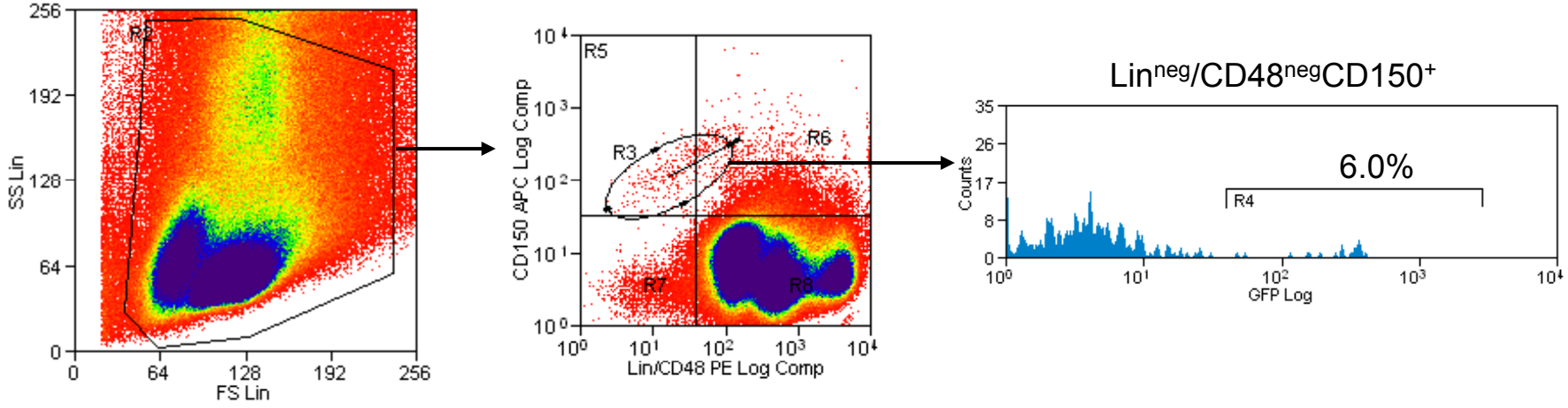

Marusyk_Suppl. Fig. S10C

C/ICN + C-comp

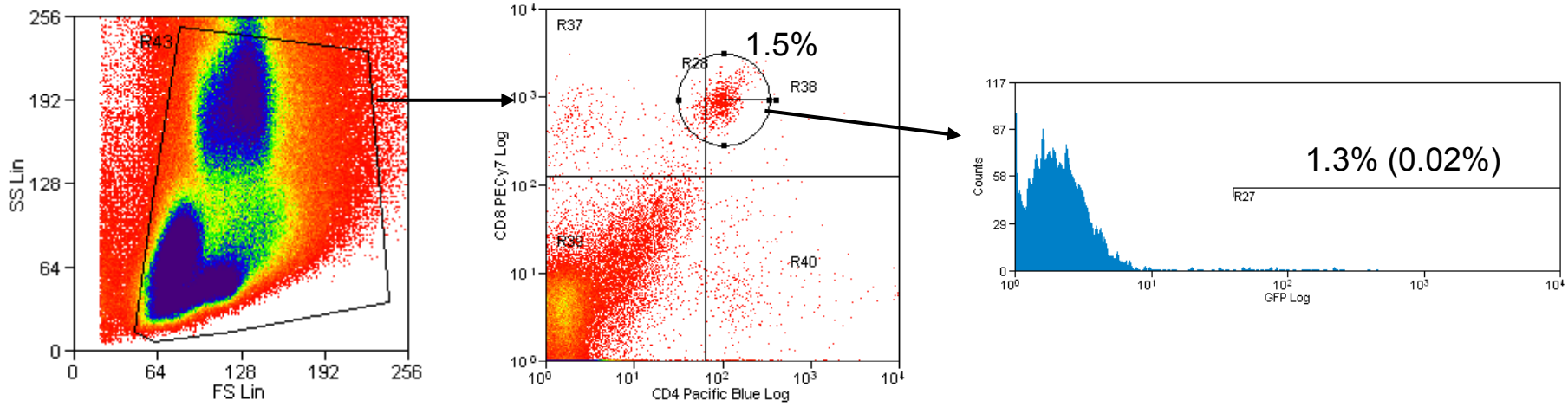

C/ICN + IR-comp

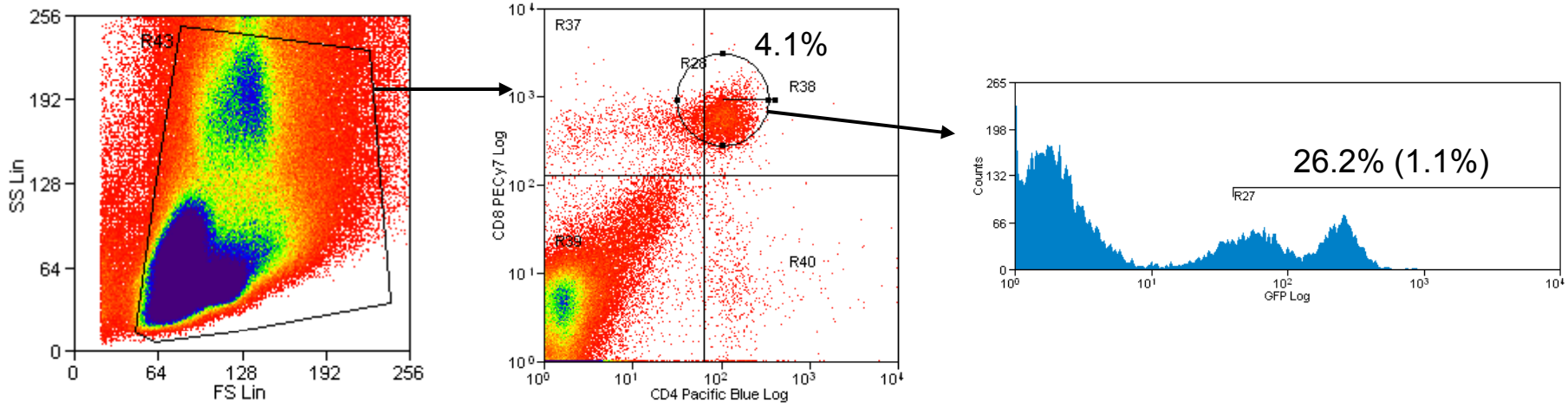

Marusyk_Suppl. Fig.S10D

IR/ICN + C-comp

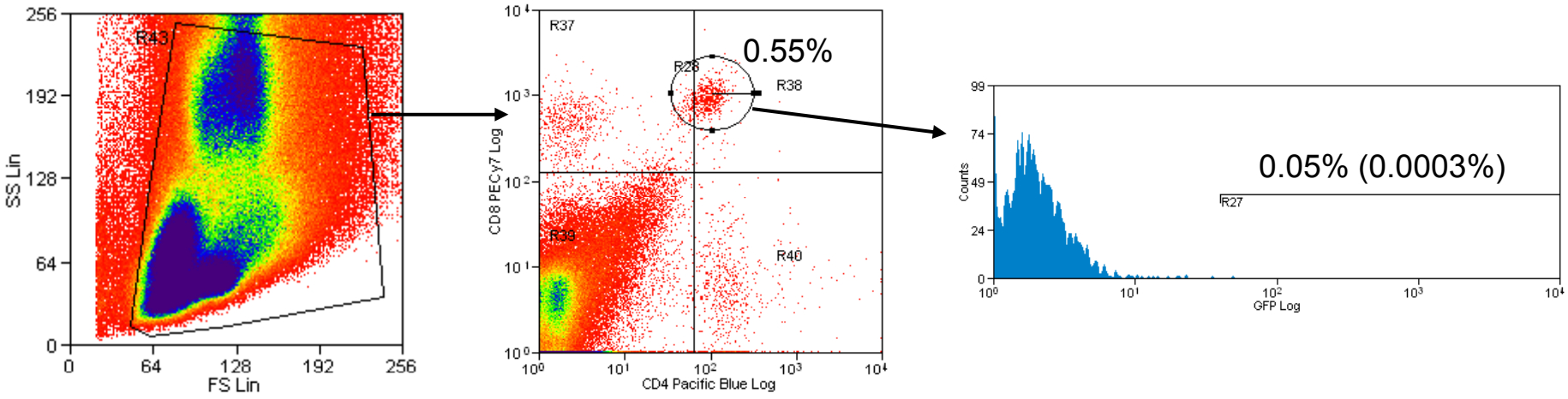

IR/ICN + IR-comp

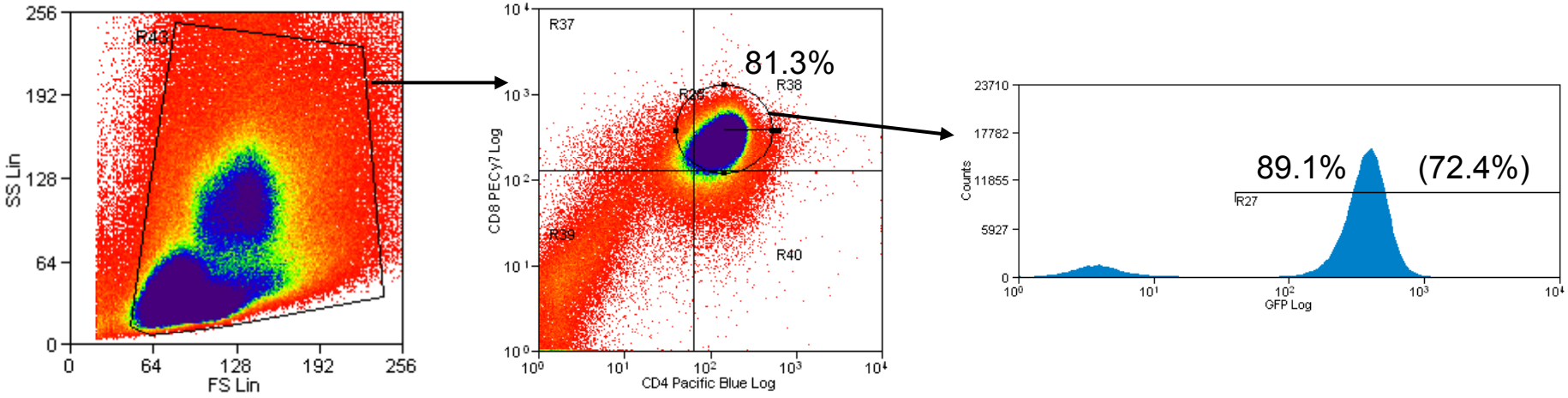

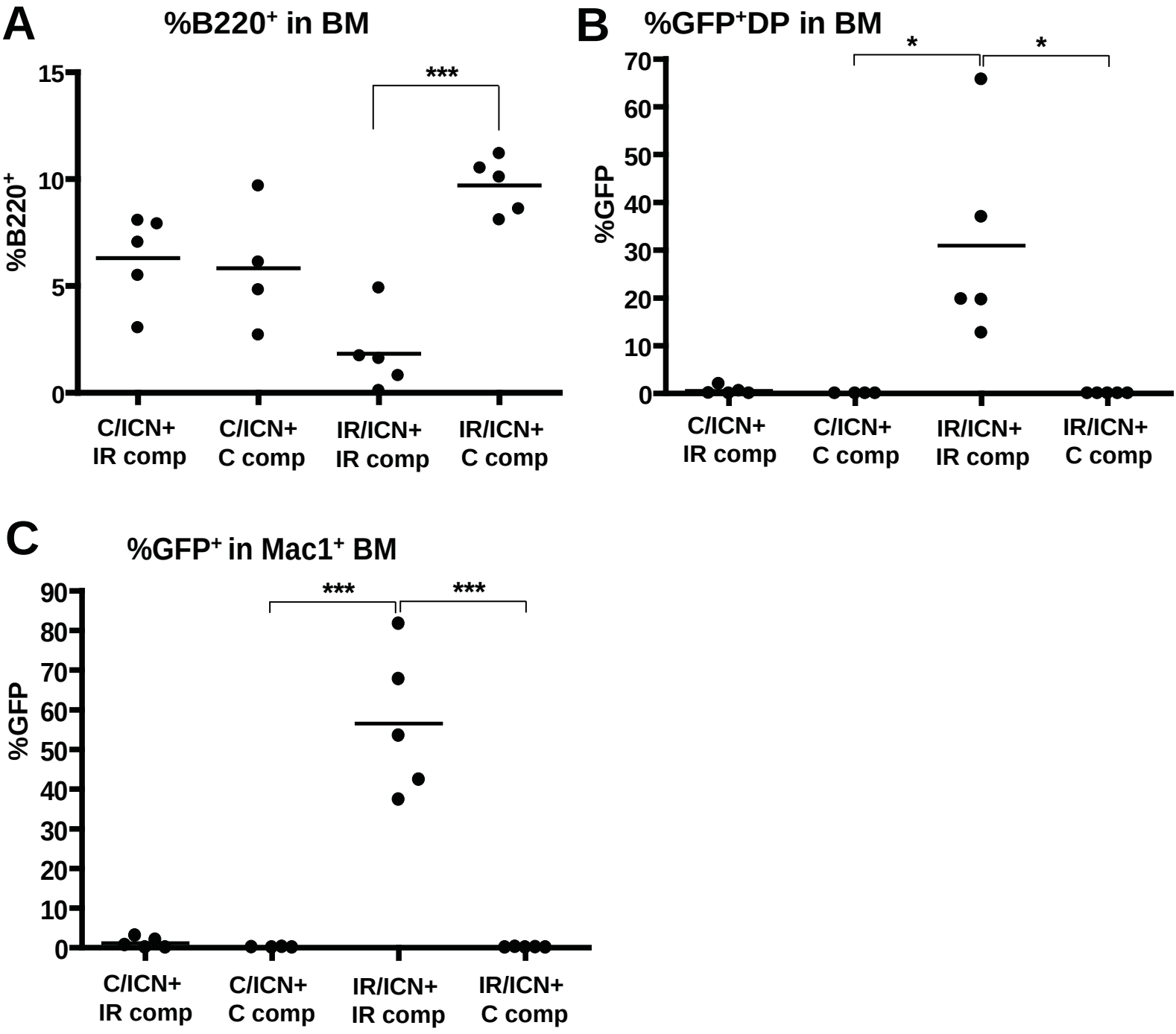
A
%B220+ in BM
%B220+
15
10
5
0
***
C/ICN+ IR comp
C/ICN+ C comp
IR/ICN+ IR comp
IR/ICN+ C comp
B
%GFP+DP in BM
%GFP
70
60
50
40
30
20
10
0
*
*
C/ICN+ IR comp
C/ICN+ C comp
IR/ICN+ IR comp
IR/ICN+ C comp
C
%GFP+ in Mac1+ BM
%GFP
90
80
70
60
50
40
30
20
10
0
***
***
C/ICN+ IR comp
C/ICN+ C comp
IR/ICN+ IR comp
IR/ICN+ C comp